1965 Microwave Transmission System Conference of the Institute of Electr. Commun. Eng. of Japan.
[5] S. Yamamoto, T. Azakami, and K. Itakura, "Coupled strip transmission line with three center conductors," *IEEE Trans. Microwave Theory Tech.*, vol. MTT-14, pp. 446–461, October 1966.
[6] H. Uchida, *Fundamentals of Coupled Lines and Multiwire Antennas.* Sendai, Japan: Sasaki Printing and Publishing Company Limited, 1967.
[7] D. Pavlidis and H. L. Hartnagel, "A microwave P.S.K. pulse modulator," *AEÜ*, vol. 27, no. 10, pp. 450–451, October 1973.
[8] D. Pavlidis, H. L. Hartnagel, and K. Tomizawa, "Phase transients of injection locked Gunn oscillators for microwave pulse communication," in *Proceedings of the 4th European Microwave Conference* (Montreux, Switzerland), September 1974, pp. 318–322.
[9] R. E. Collin, *Field Theory of Guided Waves.* New York: McGraw-Hill Book Company Inc., 1960, Ch. 4.
[10] E. M. T. Jones and J. T. Bolljahn, "Coupled-strip transmission-line filters and directional couplers," *IRE Trans. Microwave Theory Tech.*, vol. MTT-4, pp. 75–81, 1956.
[11] R. Levy, "Transmission-line directional couplers for very broad-band operation," *Proc. IEE*, vol. 112, no. 3, pp. 469–476, 1965.
[12] R. R. Gupta, "Accurate impedance determination of coupled TEM conductors," *IEEE Trans. Microwave Theory Tech.*, vol. MTT-17, pp. 479–489, 1969.
[13] E. Yamashita and R. Mittra, "Variational method for the analysis of microstrip lines," *IEEE Trans. Microwave Theory Tech.*, vol. MTT-16, pp. 251–256, April 1968.
[14] J. W. Duncan, "The accuracy of finite difference solutions of Laplace's equations," *IEEE Trans. Microwave Theory Tech.*, vol. MTT-15, pp. 575–582, October 1967.
[15] T. G. Bryant and J. A. Weiss, "Tables with parameters for microstrip lines," Document No. NAPS-0087, ADI Auxiliary Publications Service, American Society of Information Sciences, New York.

General TE_{011}-Mode Waveguide Bandpass Filters

ALI E. ATIA, MEMBER, IEEE, AND ALBERT E. WILLIAMS, MEMBER, IEEE

Abstract—**A new structure for high-Q TE_{011}-mode circular waveguide cavities is introduced and shown to realize the most general bandpass-filter transfer functions. Methods of improving the mode purity and suppressing the degenerate TM_{111} mode are presented. Several experimental narrow-bandpass filters having finite attenuation poles have been constructed; their measured responses show excellent agreement with theory. Average realizable unloaded Q's of 20 000 and 16 000 have been achieved at 8 and 12 GHz, respectively.**

INTRODUCTION

MANY modern microwave communications-system applications require exacting filter specifications in terms of selectivity, midband insertion loss, gain slope, and group delay. Synthesis methods have been developed for the realization of general transfer functions in multiple-coupled cavities [1]. Successful implementations of these synthesis techniques have been demonstrated by constructing narrow-bandpass waveguide filters in dual-mode circular cavities [2], dual-mode square cavities, and single-mode rectangular cavities [3] excited in dual TE_{111}, dual TE_{101}, and single TE_{101} modes, respectively.

The gain slope and midband insertion losses of bandpass filters are closely related to the practically realizable unloaded Q's of the cavities and the fractional bandwidth of the filters. At high frequencies (centimeter through millimeter wave), the achievable unloaded Q of waveguide cavities excited in the fundamental modes can be a limiting factor in the realization of highly selective narrow-bandpass filters having small gain slopes and in-band insertion losses. Furthermore, in high-power multiplexing applications it is important to minimize the filter losses. Typically, silver-plated waveguide-cavity filters excited in the fundamental mode can be realized with average unloaded Q's of about 10 000 at S band. At higher frequencies, lower unloaded Q's are realized due to the $1/\sqrt{f}$ dependence. For example, Q's ranging from 7000 to 5500 are achieved at X band.

An obvious way of obtaining a higher unloaded Q is to employ a higher order cavity mode, although care must be taken to ensure satisfactory cavity tuning control and suppression of adjacent modes. One mode which has been successfully employed is the circular TE_{011} mode. Known realizations of this mode are cascaded (direct-coupled) structures [4] which limit the class of transfer functions that can be realized to all-pole functions (e.g., Chebychev and Butterworth). More general characteristics, e.g., functions possessing transmission zeros at finite frequencies and nonminimum phase functions, cannot be realized in these simple direct-coupled structures.

This paper demonstrates the realization of the most general filter transfer functions in waveguide structures excited in the high-Q TE_{011} mode. It is well known that this can only be achieved if couplings among certain non-cascaded cavities are realized with arbitrary signs. A new structure satisfying the canonical form of multiple-coupled cavity realization [1] is introduced.

One of the difficulties encountered in the utilization of the TE_{011} circular waveguide-cavity mode for filter realization is the presence of the degenerate TM_{111} mode. Methods of splitting the degeneracy of the two modes are presented,

Manuscript received January 15, 1976; revised April 5, 1976. This paper is based upon work performed in COMSAT Laboratories under the sponsorship of the Communications Satellite Corporation.
The authors are with the COMSAT Laboratories, Clarksburg, MD 20734.

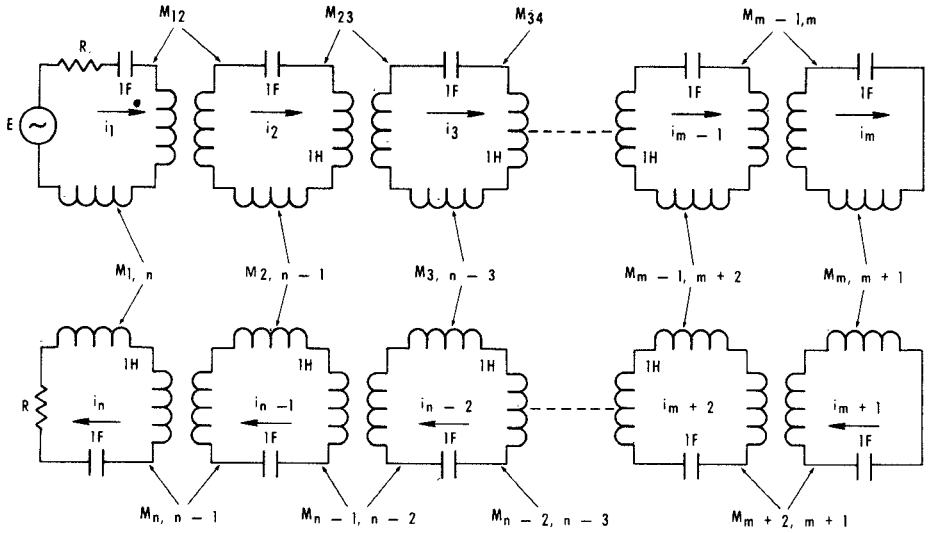

Fig. 1. Canonical form of the equivalent circuit of 2-m coupled cavities.

together with perturbation analysis of their frequency separation. Three experimental filters have been constructed and tested: two 4-cavity elliptic-function filters with center frequencies of 8.35 and 12 GHz and bandwidths of 5 and 20 MHz, respectively, and an eighth-order filter having two zeros of transmission, a center frequency of 12 GHz, and a bandwidth of 40 MHz. Experimental results for the three filters show good agreement with theory.

Theory

Synthesis and Realization

It has been shown in [1] that the most general form of symmetrical, multiple-coupled, synchronously tuned cavity networks can be reduced to the canonical equivalent circuit shown in Fig. 1. This circuit consists of two identical halves, each of which is a cascaded structure of m direct-coupled cavities having couplings of the same sign. Each cavity in one half is coupled to the corresponding cavity in the other half by an arbitrary-sign coupling element. The circuit can conveniently be described by the even (or odd) mode coupling matrix, which is a tridiagonal $m \times m$ matrix. The diagonal elements of this matrix have arbitrary signs and represent the couplings between the two symmetrical halves, while the nonzero off-diagonal elements all have the same sign and represent the direct couplings in each half. The solution to the synthesis problem, i.e., the determination of the coupling elements from a given transfer function, is treated in [1] and will not be repeated here.

To understand the realization of the canonical form of the equivalent circuit shown in Fig. 1 with TE_{011}-mode cavities, it is essential to first consider the field configuration of that mode. Fig. 2 shows a right circular cylindrical cavity and the electromagnetic-field components in the cavity for the TE_{011} mode. Two cavities excited in this mode can be coupled via the magnetic fields H_z, as in Fig. 3(a), through slots in the cavity circumference parallel to the z axis, or via the magnetic fields H_r through radial slots in the

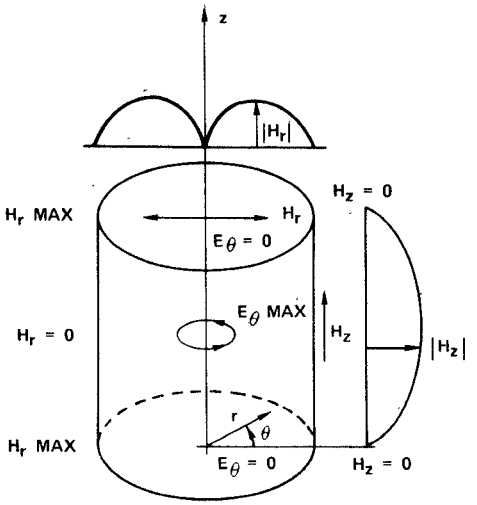

Fig. 2. Right circular cylindrical cavity showing TE_{011}-mode fields.

cavity ends. The relative sign of the radial magnetic-field coupling can be chosen as positive when the two cavities are aligned so that their axes are coincident as in Fig. 3(b). On the other hand, negative coupling results if the two cavities are offset so that their axes are parallel but separated by one-half diameter, as shown in Fig. 3(c).

As described in the literature, previous filters utilizing the TE_{011} mode [4] have consisted of the structures shown in Fig. 4(a) and (b), which utilize both kinds of coupling slots shown in Fig. 3(a) and (b). The couplings realizable by these structures are all of the same sign. Since the general canonical form of the equivalent circuit requires both negative and positive couplings, the structures of Fig. 4(a) and (b) cannot realize the most general characteristics. Fig. 4(c), on the other hand, shows how negative couplings in the canonical form can be realized. The overlapping cavities at half-diameters coupled by radial slots produce the negative-coupling elements, while all the other slots produce positive couplings. It should be noted that the

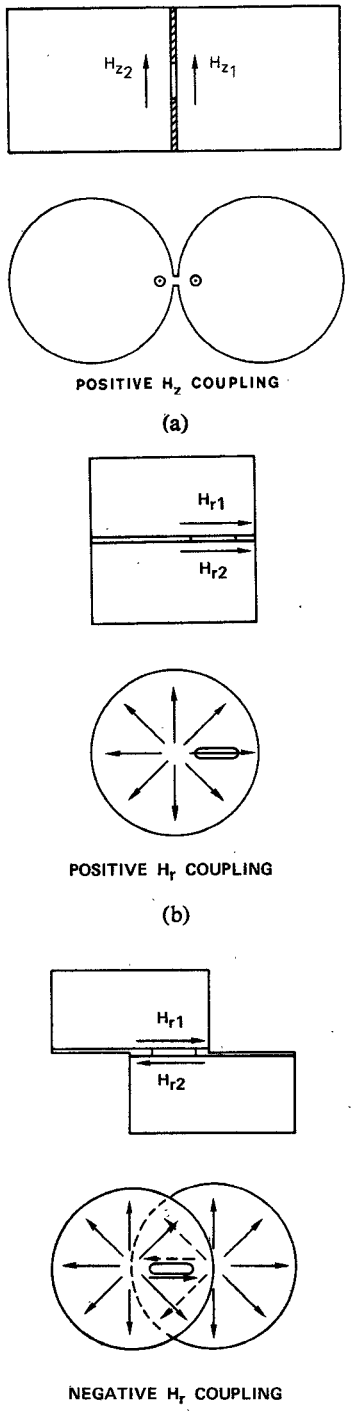

Fig. 3. Possible methods of coupling two cavities excited in the TE_{011} mode. (a) Axial circumferential slot (H_z) coupling. (b) Radial slot in base or top (H_r) positive coupling. (c) Radial slot in base or top (H_r) negative coupling.

labeling of signs is important only in indicating that "shunt" coupling elements can have different signs for an adjacent pair of cavities. The basic building block of this new realization is therefore a set of four electrical cavities whose implementation as a fourth-order elliptic transfer function would be sufficient confirmation of the properties of the general structure.

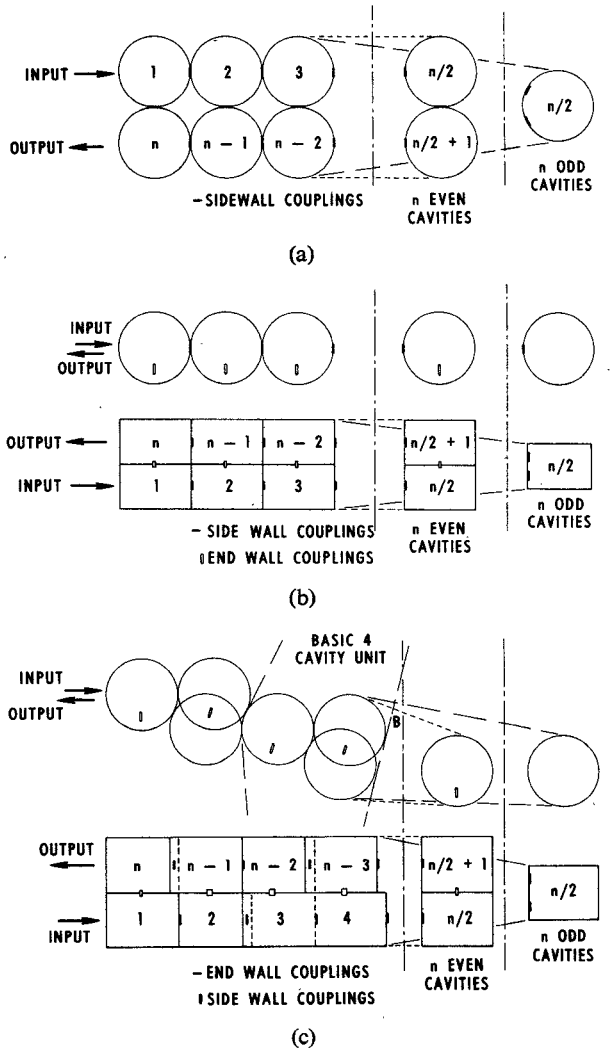

Fig. 4. (a) TE_{011}-mode filter with sidewall couplings ("shunt" couplings all $+ve$ or all $-ve$). (b) TE_{011}-mode filter with sidewall and endwall couplings ("shunt" couplings all $+ve$ or all $-ve$). (c) TE_{011}-mode filter with sidewall and endwall couplings ("shunt" couplings may be $+ve$ or $-ve$).

Mode Purity Control

One of the major problems encountered in the utilization of higher order modes in waveguide cavities is that of controlling other modes which have resonant frequencies close to or degenerate with the desired mode. The effect of the nondegenerate modes can usually be minimized by the proper choice of cavity dimensions. For example, consider the problem of determining the best dimensions for a 12-GHz cavity to be excited in the TE_{011} mode. In Fig. 5, which is a "mode chart" [4] for a cylindrical cavity of 1.4-in diameter, the resonant frequencies of the different modes are plotted versus cavity length. Except for the degenerate TM_{111} mode, it can be seen that selecting a cavity length of 0.93 in will give the required 12-GHz resonant frequency with the nearest modes being the TE_{311} and TE_{211} modes resonating at 13.1 and 10.6 GHz, respectively. Different mode charts can be plotted for different diameters and the proper dimension can be selected on the basis of the relative

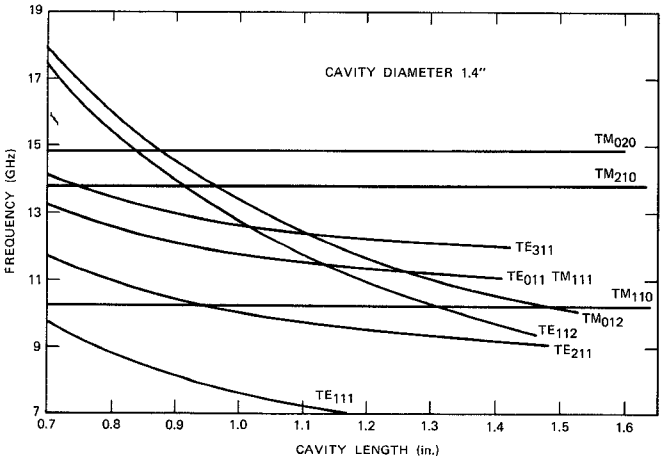

Fig. 5. Mode chart for a 1.4-in-diam cylindrical cavity.

TABLE I
ELECTROMAGNETIC-FIELD COMPONENTS IN AN UNPERTURBED CAVITY OF LENGTH L AND DIAMETER D

Field Component	TE_{011} Mode	TM_{111} Mode
E_r	0	$-\frac{k_3}{k} J_1'(k_1 r) \cos\theta \sin k_3 z$
E_θ	$j\eta J_0'(k_1 r) \sin k_3 z$	$\frac{k_3}{k} \frac{J_1(k_1 r)}{k_1 r} \sin\theta \sin k_3 z$
E_z	0	$\frac{k_1}{k} J_1(k_1 r) \cos\theta \cos k_3 z$
H_r	$\frac{k_3}{k} J_0'(k_1 r) \cos k_3 z$	$-\frac{j}{\eta} \frac{J_1(k_1 r)}{k_1 r} \sin\theta \cos k_3 z$
H_θ	0	$-\frac{j}{\eta} J_1'(k_1 r) \cos\theta \cos k_3 z$
H_z	$\frac{k_1}{k} J_0(k_1 r) \sin k_3 z$	0

importance of the frequency band in which higher order modes occur.

For successful filter realization, the degenerate TM_{111} mode must be suppressed so that no energy is transferred to or absorbed in its resonance. The degeneracy of the TM_{111} mode can be split by introducing proper perturbations in the cavity. Since the TE_{011} mode has no longitudinal currents in the cavity walls, a noncontacting tuning plunger [4] can be used without appreciably degrading its unloaded Q, and at the same time, it can shift the resonant frequency of the TM_{111} mode to a lower frequency.

Two other methods of further increasing the TM_{111}-mode suppression have been considered. First, a thin dielectric coating on the tuning plunger can be used to shift the resonant frequency of the TM_{111} mode to a lower frequency. Since the electric field of the TE_{011} mode is zero at the plunger's position, no change in its resonance or unloaded Q should occur. Second, a set of "tuning posts" can be introduced at proper locations in the tuning plunger to achieve a similar effect. The quantitative effects of both of these methods on the resulting frequency shift between the TE_{011} and TM_{111} modes can be estimated by carrying out a simple perturbation analysis for both modes. The electromagnetic-field components of both modes that would exist in an unperturbed cavity of length L and diameter D are given in Table I [5], where $k_1 = 7.664/D$, $k_3 = \pi/L$, $k = 2\pi/\lambda$, $k^2 = k_1^2 + k_3^2$, $\eta = \sqrt{\mu_0/\varepsilon_0}$ is the free-space intrinsic impedance, and J_0 and J_1 are the Bessel functions of orders zero and one, respectively.

If a thin dielectric coating of thickness t and relative dielectric constant ε_r is placed on the tuning plunger, then only the TM_{111} mode is affected, and its resonant frequency will be lowered by [6]

$$\frac{\omega - \omega_0}{\omega} = -(\varepsilon_r - 1) \frac{\iiint_{\Delta v} \varepsilon_0 |\bar{E}_0|^2 \, dv}{4U_{\text{total}}}. \quad (1)$$

On the other hand, a small conducting post of volume Δv placed on the plunger will shift the resonant frequencies of both modes from their nominal values by [6]

$$\frac{\omega - \omega_0}{\omega} = -C \frac{\iiint_{\Delta v} (\varepsilon_0 |\bar{E}_0|^2 - \mu_0 |\bar{H}_0|^2) \, dv}{4U_{\text{total}}}. \quad (2)$$

In (1) and (2) $\bar{E}_0$ and $\bar{H}_0$ are the fields which would exist at the disturbing samples positions if the perturbations were not present, and U_{total} is the total energy stored in the cavity for the fields of the corresponding mode. The constant C in (2) is a "magnification factor" which is introduced to accommodate the presence of sharp edges in the perturbing samples [7]. It is known that, at sharp conducting edges, certain field components can have singular behavior and increase to large values. These singularities increase significantly the amount of resonant-frequency shift relative to that predicted by the perturbation analysis assuming smooth perturbing objects, for which the factor C in (2) is unity. Sharp edges in the perturbing samples result in large values of C.

When the fields of Table I are substituted in (1) and (2) and the integrations are carried out, the resulting frequency shifts between the two modes for the respective cases can be shown to be

$$\frac{\Delta\omega}{\omega_0} = 0.295(1 - \varepsilon_r) \left(\frac{\lambda}{D}\right)^2 \left(\frac{t}{L}\right) \quad (3a)$$

for a dielectric-coated plunger, and

$$\frac{\Delta\omega}{\omega_0} = 1.97C \frac{\Delta V}{D^2 L} [f(k_1 r_0) + \cos 2\theta_0 g(k_1 r_0)] \quad (3b)$$

for a conducting post at position (r_0, θ_0, L) in the plunger, where

$$f(x) = J_1^2(x) - \tfrac{1}{2}\{J_0^2(x) + J_2^2(x)\} \quad (4)$$

$$g(x) = \left(\frac{k_1}{k}\right)^2 J_1^2(x) + J_0(x) J_2(x). \quad (5)$$

From (3b) it is clear that the frequency shift of the two modes depends upon the angular position θ_0, and radial position r_0 of the post in the tuning plunger. To simplify the practical implementation of the plunger, it is desirable to

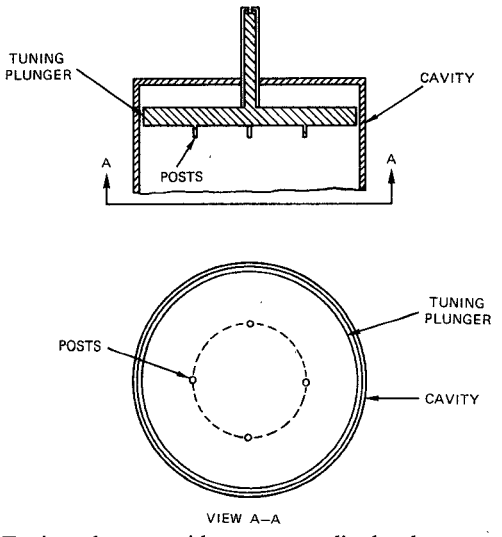

Fig. 6. Tuning plungers with posts to split the degeneracy of the TE_{011} and TM_{111} modes.

eliminate the angular dependence of the frequency shift. This can be accomplished by having either two or four posts separated by 90° angular intervals and at the same radial location, as shown in Fig. 6. With this configuration, the frequency shift between the TE_{011} and TM_{111} modes can be made independent of the angular orientation of the tuning plunger, since the $\cos 2\theta_0$ terms in (3b) will cancel out.

It can be seen that the function $f(x)$ has a minimum of -0.5 at $x = 0$ and that its maximum of 0.246 occurs at $x = 1.97$, i.e., $r_0 = 0.257D$. Although a single post at the center of the plunger would appear to produce about twice the frequency shift produced by a post of the same volume placed at approximately one-half radius, the latter is preferable to the former for two reasons. First, it has a frequency shift of the same sign as that caused by the gap between the noncontacting plungers and the cavity walls. Second, and more importantly, since the perturbation is predominantly in the electric field of the TM_{111} mode, the factor C is much larger for a post placed at one-half radius than for a post in the center of the plunger, which appears as a smooth object for the magnetic fields of the modes.

Practical implementations of both the dielectric-coated plungers and the tuning posts were found to split the degeneracy of the modes. Computed frequency shifts from (3a) for dielectric-coated plungers corresponded closely to measured values. For tuning posts at one-half radius, the measured frequency shifts were found to correspond to those predicted from (3b) with the factor C approximately 40. In both cases the unloaded Q's of the TE_{011} mode were not degraded appreciably.

Experimental Results

To demonstrate that a negative coupling (or an appropriate sign-coupling set) in the TE_{011}-mode cavity structure can be generated, a 12-GHz 4-cavity filter with an

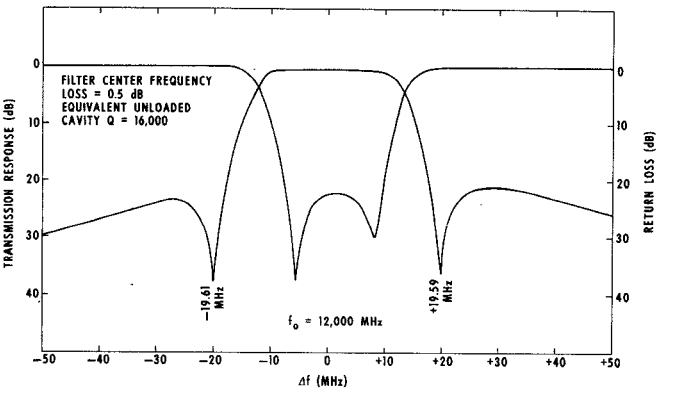

Fig. 7. Insertion- and return-loss response of 12-GHz 4-cavity filter.

elliptic transfer function was designed. Modal purity was achieved, first by judicious selection of the cavity dimensions (see Fig. 5) and second by using slightly different cavity diameters so that the lower and higher order modes of adjacent cavities resonated at slightly different frequencies. This in turn reduced the energy coupled between these resonances and the out-of-band transmission responses. Cavity-coupling slot dimensions were determined by using the small-aperture coupling theory described by Bethe and modified for larger apertures by Cohn [8]. The dimensions were then adjusted experimentally by employing the coupling measurement technique described in [9].

The measured experimental response for this filter is shown in Fig. 7. The center-frequency loss of 0.5 dB corresponds to an average unloaded Q of 16000. The realization of the two real zeros of transmission confirms that an opposite-sign shunt-coupling set has been achieved and that the general TE_{011} filter structure of Fig. 4(c) is correct.

The techniques described in the previous section for splitting the degeneracy of the TE_{011} and TM_{111} modes have both been used in the 12-GHz filter. The wide-band frequency transmission responses are shown in Figs. 8 and 9, where the spurious responses are identified as lower and higher order modes of the cylindrical cavity. The dielectric-loaded plungers were constructed with a 0.033-in-thick coating of Teflon. The frequency shift of the TM_{111} mode as predicted by (3a) is approximately 70 MHz, while a shift of about 100 MHz has been obtained experimentally. On the other hand, the frequency shift produced by the tuning stubs has been measured experimentally to be 300 MHz, which corresponds to a magnification factor (C) of 40 as computed from (3b). To obtain the same performance using dielectric plungers, a Teflon thickness of 0.10 in is required, which causes a large degradation in Q. Consequently, the tuning-stub plunger design is preferable to dielectric loading. Fig. 10 is a photograph of the 12-GHz 4-pole elliptic function filter.

Further confirmation of the validity of the 4-cavity filter unit and its design has been provided by an extremely narrow-bandpass (5-MHz) elliptic filter centered at 8.35

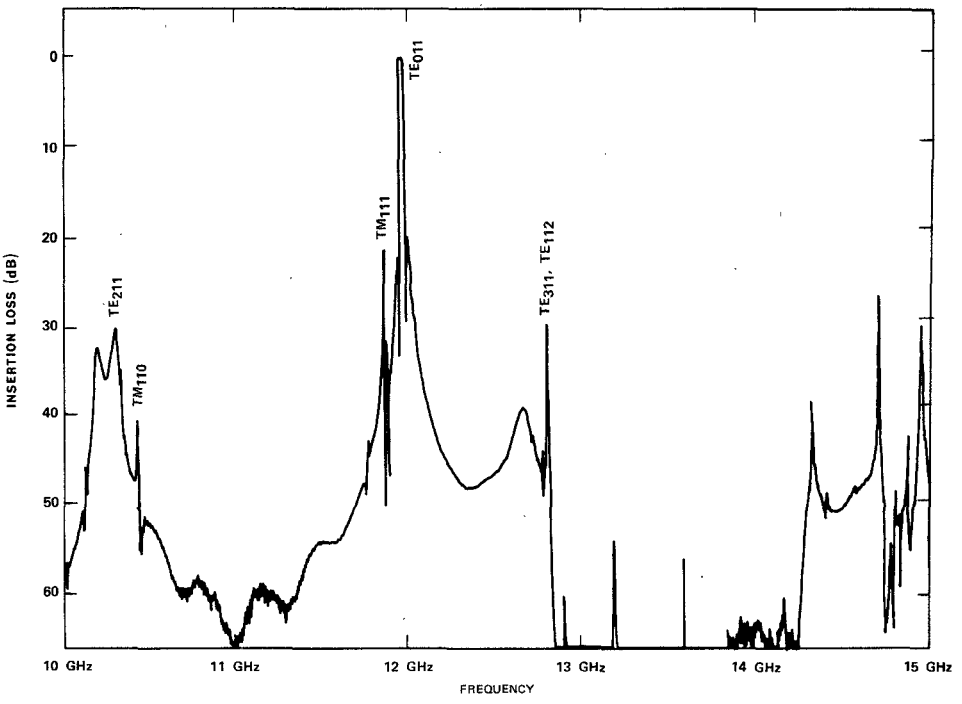

Fig. 8. Wide-band insertion-loss sweep of 4-pole 12-GHz filter, Teflon-coated plungers.

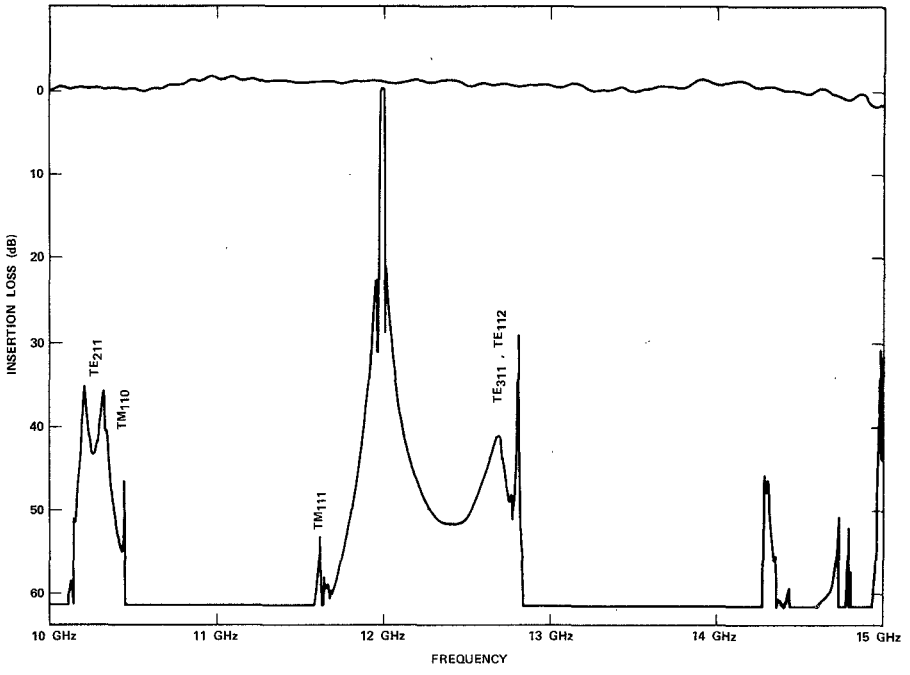

Fig. 9. Wide-band insertion-loss sweep of 4-pole 12-GHz filter, post-tuned plungers.

GHz. The measured transmission and return losses are shown in Fig. 11, with the midband insertion loss of 1.25 dB corresponding to an unloaded Q of 20000. No spurious responses were present over a band of 700 MHz around center frequency. The tuning-stub plunger design has effectively suppressed the degenerate TM_{111} mode.

The 4-cavity experimental filters demonstrate first that the general filter concepts are correct and second that mode purity can be controlled by careful choice of cavity dimensions and plunger design. An example of a more complex filter is provided by the synthesis and realization of an 8-cavity 12-GHz filter having four zeros of transmis-

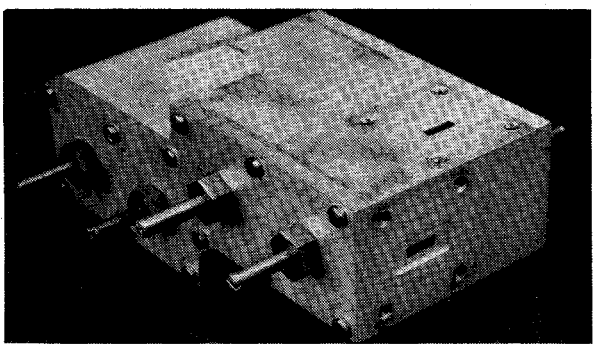

Fig. 10. Photograph of 12-GHz 4-cavity filter.

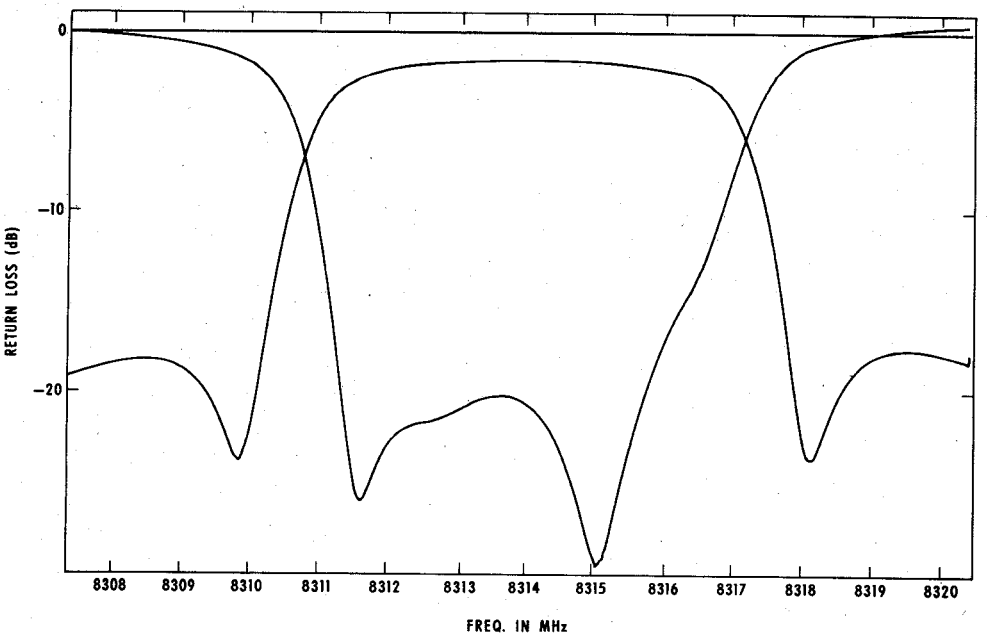

Fig. 11. Insertion- and return-loss responses of 8.35-GHz filter.

sion and a 0.05-dB equiripple bandwidth of 40 MHz. This filter has been designed from the low-pass normalized transfer function $t(\lambda)$ given by

$$|t(\lambda)|^2 = \frac{1}{1 + \varepsilon^2\phi^2(\lambda)} \tag{6}$$

where

$$\phi(\lambda) = \frac{(\lambda^2 - z_1^2)(\lambda^2 - z_2^2)(\lambda^2 - z_3^2)}{(\lambda^2 - P_1^2)(\lambda^2 - P_2^2)} \tag{7}$$

with $z_1 = 0.6086$, $z_2 = 0.8765$, $z_3 = 0.9875$, $P_1 = 1.2388$, and $P_2 = 1.4346$.

The synthesis procedure of [1] has been used to evaluate the normalized couplings of the canonical form of the equivalent circuit as an even-mode coupling matrix having the form

$$M = \begin{bmatrix} 0 & 0.9184 & 0 & 0 \\ 0.9184 & 0.0546 & 0.6213 & 0 \\ 0 & 0.6213 & -0.3330 & 0.4747 \\ 0 & 0 & 0.4747 & 0.8240 \end{bmatrix}. \tag{8}$$

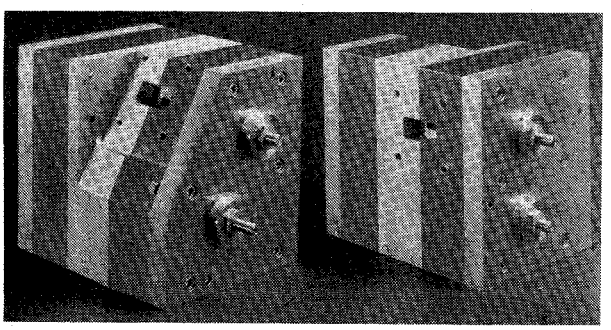

Fig. 12. Photograph of 12-GHz 8-cavity filter.

This coupling matrix has been realized in the filter structure shown in Fig. 12. The measured frequency response of the transmission and return loss is compared to the theoretical response in Fig. 13. The midband insertion loss of 0.7 dB corresponds to an average unloaded Q of 16000. The agreement between theory and experiment is good. Out-of-band resonances are shown in Fig. 14. The TM_{111} mode is completely suppressed by the posts in the tuning plungers.

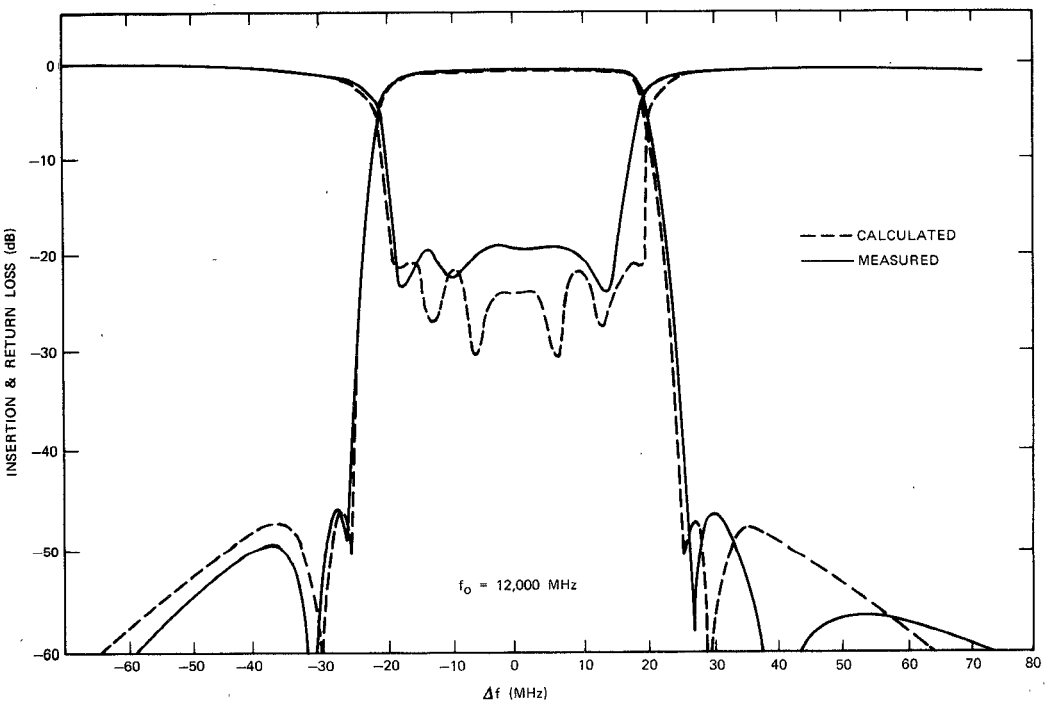

Fig. 13. Measured and computed insertion and return losses of 8-cavity filter.

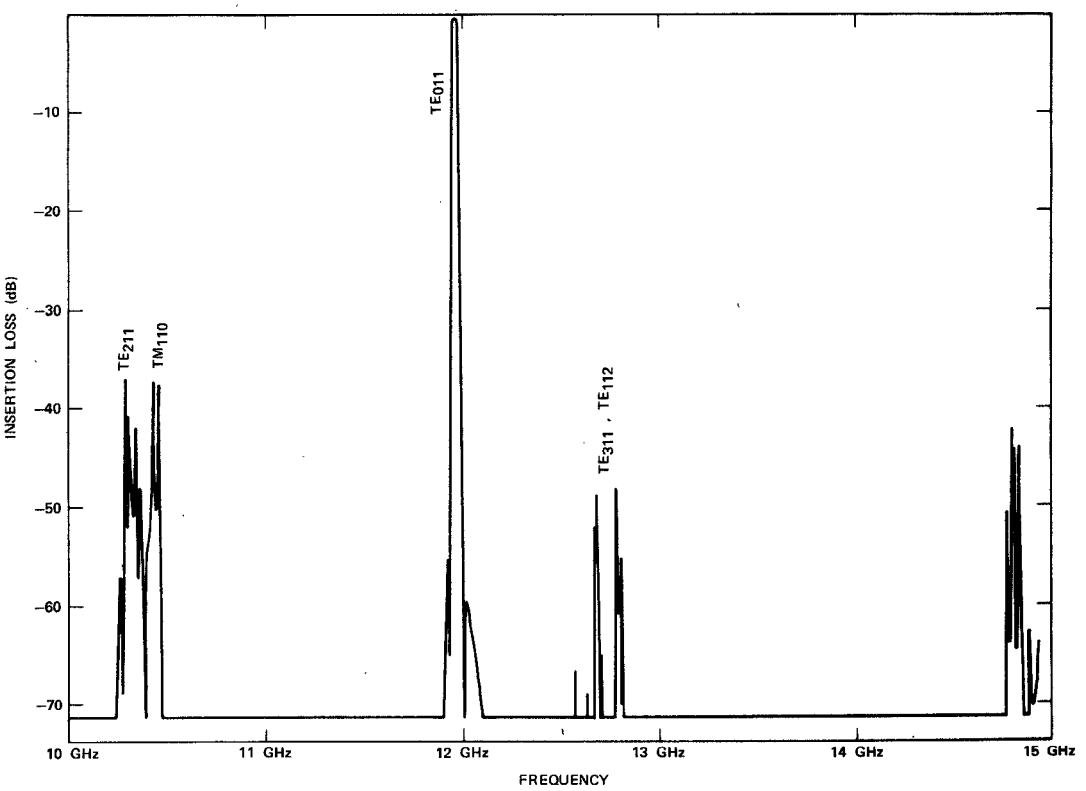

Fig. 14. Wide-band frequency sweep of 8-cavity filter.

Discussion and Conclusions

This paper has shown how to construct general TE_{011}-mode circular-waveguide filters by demonstrating (theoretically and practically) the realization of both positive and negative coupling elements in a canonical form. The experimental filter responses indicate excellent agreement with theory. It has been shown that the degenerate TM_{111} mode can be effectively suppressed, and a suppression method has been analyzed and successfully implemented in the experimental filters. Finally, a method for temperature compensation of TE_{011}-mode cavities will be described in an accompanying paper [10]. This technique enables lightweight thermally stable bandpass filters to be constructed from aluminum instead of Invar and/or graphite-reinforced fibers. Significant savings in weight and cost of fabrication are therefore achieved.

Acknowledgment

The authors wish to thank R. W. Kreutel and W. Getsinger for their encouragement and support in the course of this work, and R. Kessler for coordinating the construction of the three experimental filters.

References

[1] A. E. Atia, A. E. Williams, and R. W. Newcomb, "Narrowband multiple coupled cavity synthesis," *IEEE Trans. Circuits and Systems*, vol. CAS-21, no. 5, September 1974.
[2] A. E. Atia and A. E. Williams, "Narrow bandpass waveguide filters," *IEEE Trans. Microwave Theory and Techniques*, vol. MTT-20, pp. 258–265, April 1972.
[3] ——, "Non-minimum phase, optimum amplitude bandpass waveguide filters," *IEEE Trans. Microwave Theory and Techniques*, vol. MTT-22, pp. 425–431, April 1974.
[4] G. L. Matthaei, L. Young, and E. M. T. Jones, *Microwave Filters, Impedance Matching Networks and Coupling Structures.* New York: McGraw-Hill, 1965, ch. 15.
[5] *Techniques of Microwave Measurements*, C. G. Montgomery, Ed. Radiation Laboratory Series, vol. 11. New York: McGraw-Hill, 1949, p. 385.
[6] J. Altman, *Microwave Circuits.* New Jersey: D. Van Nostrand Co., 1964, pp. 409–416.
[7] E. L. Ginzton, *Microwave Measurements.* New York: McGraw-Hill, 1957, pp. 439–452.
[8] S. B. Cohn, "Microwave coupling by large apertures," *Proc. IRE*, vol. 40, pp. 696–699, June 1952.
[9] A. E. Atia and A. E. Williams, "Measurements of intercavity couplings," *IEEE Trans. Microwave Theory and Techniques*, vol. MTT-23, pp. 519–522, June 1975.
[10] ——, "Temperature compensation of TE_{011}-mode circular cavities," *IEEE Trans. Microwave Theory and Techniques*, this issue, pp. 668–669.

Short Papers

A Discriminator-Stabilized Microstrip Oscillator

B. GLANCE, MEMBER, IEEE, AND W. W. SNELL, JR.

Abstract—**A 5.2-GHz microstrip Gunn oscillator has been frequency stabilized by means of a novel microstrip discriminator and integrated feedback loop. A stabilization factor of 1000 was measured for the oscillator with an external Q of 50. The self-capture bandwidth of the discriminator circuit is large enough to eliminate the need for a search voltage to obtain initial frequency locking.**

I. Introduction

Solid-state oscillators have a relatively low-frequency stability and require frequency stabilization in order to be used as signal sources in radio communication systems. The purpose of this short paper is to describe a stabilization technique which is suited to microstrip oscillators. Stabilization can be achieved by several techniques, such as, frequency or phase locking to a stable reference signal, locking to a high-Q cavity, or by use of a discriminator circuit. Among these techniques, the discriminator scheme offers the possibility of a simpler and less costly stabilization circuit by using microstrip technology. A new thin-film discriminator is proposed in this short paper which can be readily integrated with a microstrip oscillator to provide high-frequency stability.

Manuscript received December 19, 1975; revised April 15, 1976.
The authors are with the Crawford Hill Laboratory, Bell Laboratories, Holmdel, NJ 07733.

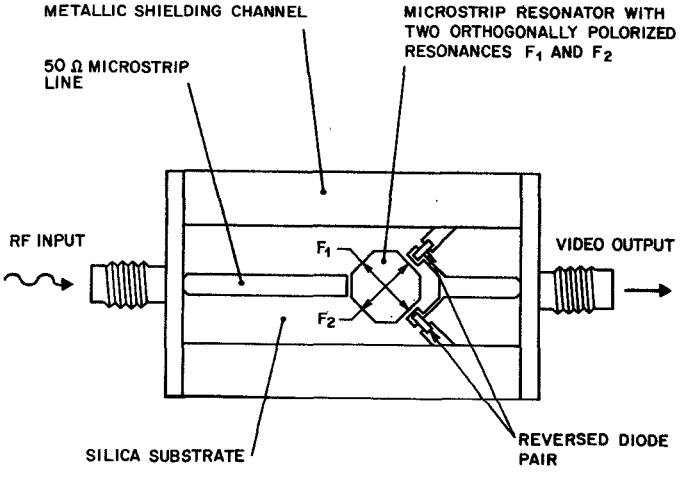

Fig. 1. Circuit configuration of the microstrip discriminator showing how each diode is capacitively coupled to one of the two orthogonal modes of the microstrip resonator.

II. Microstrip Discriminator

The thin-film discriminator is shown in Fig. 1. It consists of a double-mode microstrip resonator with a pair of detector diodes. The resonator has the geometrical shape of a rectangle with truncated corners and its electrical properties are similar to the resonator used in a recently developed thin-film millimeter-wave downconverter [1], [2]. The RF input signal excites two ortho-